

THE MECHANICAL PROPERTIES OF MEDIUM DENSITY RIGID POLYURETHANE BIOFOAM

Ernie Suzana Ali^{1,a} and Syazana Ahmad Zubir²

¹Applied Physic Programme, Faculty of Science and Technology, Universiti Sains Islam Malaysia, 71800 Nilai, Negeri Sembilan, Malaysia

²Pusat Pengajian Kejuruteraan Bahan Dan Sumber Mineral, Kampus Kejuruteraan, Universiti Sains Malaysia, 14300 Nibong Tebal, Seberang Prai, Pulau Pinang, Malaysia

Abstract. This paper described the effect of empty fruit bunch (EFB) loading in the medium density rigid foam, which was prepared from the palm kernel oil based polyol. The grounded 300 μ m EFB fiber was used as filler and its composition were varied from 3, 6, 9 and 12 weight percent. EFB filled PU shown good dimensional stability at 70 $^{\circ}$ C and -15 $^{\circ}$ C due expanding and shrinking percentage are less than 0.8% and 0.4% respectively. The mechanical properties were increased linearly with the EFB loading until it reached an optimum percentage of the EFB. SEM images shows the usage of big size cylindrical particle suggested that the fiber pull out will responsible for the synergistic effect of flexibility and strength of the biofoam produced.

1 Introduction

Polyurethane is used in various branches of industry such as foams, elastomers and coatings because of their unique combination of good characteristics with various special properties [1, 2]. Polyurethane foams can be assumed composite structures resulting by the controlled entrapment gases that are generated during the polymerization between polyisocyanates and polyfunctional alcohols to form urethane linkage.

Recently, most commercially available polyols are petrochemical-based. There has been an interest to find alternative sources for raw materials to be used in the production of polyols. A number of researchers have investigated the possibilities at converting vegetable oil into polyols for polyurethane foams [2, 3]. Much attention is paid to introducing plant resources into polyurethane foam production. The materials prepared from biomass not only open a new and efficient way to use regeneratable natural resources, but also possess a great potential for bio and photo degradability [4]. The latter advantage is more striking in the urgent need of environmental protection [4].

Palmeri oil, vernonia oil, castor oil, cardanol oil and soy oil have been synthesized with multiple functionality, an alternative to replace the petrochemical based polyols [5, 6, 7]. Badri et. al has used palm kernel oil (PKO) in producing low functionality polyol and high functionality polyol with insertion sorbitol as an additive [8]. In the production of polyurethane with the PKO polyol based, we used water as a blowing agent as an alternative to prevent our ozone while using CFC [6].

Fillers have always played an important role in the plastic industry. The utilization of lignocellulosic materials in making composites has received considerable attention, in recent times particularly in thermoplastic composites [5, 7, 8]. This has been attributed to several advantages offered by lignocelluloses fillers, such as lower density, greater deformability, less abrasiveness to equipment, biodegradability and lower cost [9, 10]. Xiaoya C. et. al [11], 1998 had used bamboo fiber and polypropylene in producing wood composite. Rozman [9] also had used EFB as a filler and poly-ethyl-glycol (PEG) as a matrix in producing polyurethane rigid foam.

In order to maintain Malaysian leading position in palm oil industry, by-products of this industry, such as EFB, palm shells, pressed fruit fibers and palm oil mill effluent should be utilized effectively. In this study, the polyol used is derived from PKO using polycondensation method [6]. The reinforcing fillers used in this study was also derived from palm oil tree component namely EFB. The EFB waste generated by the industry is estimated to be about 8 x 10⁶ tons per year [9, 10].

2 Materials and Method

2.1 Materials

The EFB in fiber form was supplied by Sabutek Sdn. Bhd., Teluk Intan, Perak. The RBD palm kernel oil was obtained from Lee Oilmill Sdn. Bhd, Klang was used without any purification. The hydroxyl component was obtained from diethanolamine (DEA) supplied by Cosmopolyurethane (M) Sdn. Bhd, Pelabuhan Klang.

^a Corresponding author: ernie@usim.edu.my

The alkaline catalyst, potassium acetate in monoethylene glycol was supplied by Air Products Inc., Hong Kong. Chemicals used to produce the polyurethane foam were surfactant Tegostab B8444 (Th. Goldschmidt, Singapore), the catalysts: tetramethylhexanediamine (TMHDA) and pentamethyldipropylenetriamine (P77) (Cosmopolyurethane (M) Sdn. Bhd, Pelabuhan Klang) and the crude MDI (2,4-diphenylmethane diisocyanate). The blowing agent was ordinary water. The synthesis of polyols from PKO was carried out according to the polycondensation method [6]. The FTIR was carried out to the polyol in monitoring the production of the polyol. The EFB was grinded using grinding machine. It was then sieved using standard Endecotts sieve to separate the particles into different sizes. The filler size used in this study was of mesh $150\mu\text{m} < x \leq 300\mu\text{m}$. The sieved fibers were then dried in a vacuum oven to a constant weight at 105°C for 20 hours [9].

2.2 Foaming process

The MDI (120 g) was poured into 100 g mixture of polyol resin (100 pbw RBD palm kernel oil polyol, 2 pbw Tegostab B8444, 0.4 pbw TMHDA, 0.4 pbw P77, 0.06 water and the EFB: 0, 3, 6, 9 and 12 % of the system). The mixture was agitated vigorously using a standard propeller with speed of 5000 rpm for 10 seconds at 20°C . The mixture was then poured into a waxed mould, covered and screwed tight. The foam was conditioned for 16 hours at room temperature and atmospheric pressure after demoulded.

2.3 Density of the PU foams

The (apparent) densities of the PU biofoams were measured according to BS4370: Part 1:1988. Total five specimens with dimensional size $50 \times 50 \times 50$ mm (length \times width \times thickness) were cut from the PU foam after moisture conditioned at 23°C , 50%RH for 24h. The density was calculated by M/V , where M refers to the mass of each specimen and V is the volume obtained from the products of length, width and thickness of specimen. The averaged density of five specimens was reported.

2.4 Mechanics properties

Compressive strength and modulus of the PU biofoams were measured according to BS4370: Part 1:1988 with compressive strain 10% and speed of crosshead movement of 2.5 mm/min. The size of the specimen was $50 \times 50 \times 50$ mm (width \times length \times thickness) after moisture conditioned at 23°C , 50%RH for 24h. The foam rise direction was marked and a crosshead speed of 50 mm/min was applied. The averaged compressive strength and modulus of five specimens was reported. The tensile test was carried out on 'dumbbell' shaped specimen according to ASTM D638 type-V at room temperature using Universal Testing Machine model Instron 5567. The load cell used was 1 kN at a strain rate of 5 mm/min. The averaged tensile strength and modulus of five

specimens was reported. The three point bending test was done according to ASTM D790. Bending samples ($10 \times 13 \times 190$ mm). were test using Universal Testing Machine model Instron 5567 at compression speed of 4.1 mm/min and the averaged modulus of elasticity (MOE) and modulus of rupture (MOR) of five specimens was reported. Izod impact test were carried out according to ASTM D 256-91 using Universal Pendulum Impact System. The molded plates were mould into Izod impact bars ($12.7 \times 60 \times 127$ mm) and impact strength of five specimens were reported.

2.5 Dimensional stability

The dimensional stabilities of PU foams were determined according to BS4370: Part 1:1988. The dimensional size of testing specimens were $100 \text{ mm} \times 100 \text{ mm} \times 25 \text{ mm}$ after moisture conditioned at 23°C , 50%RH for 24hrs. The lengths, widths and thicknesses of specimen before and after kept for 24 hrs at -15°C and 70°C , respectively, were measured. The dimensional stabilities characterized by dimensional swelling at 70°C and dimensional shrinkage at -15°C .

2.6 Morphology of the PU biofoams

Philips XL-30 scanning electron microscope was applied to observe the morphologies of the PU foams. All SEM samples were coated with approximately 10–20 nm of gold before SEM examination.

3 Results and Discussions

Properties of the medium density biofoam produced were tabulated in Table 1. Since the specimens prepared for testing have to be in the core density range of 165-170 kg/m^3 , an excess amount of water was required as weight percentage of EFB increased. The addition of water resulted in dilution of the whole resin system that means dilution of the standard catalysts used. However, there is a trend where the optimum fiber loading exhibited a slower reaction, giving enough time for the formation of the cellular structure of the foam. The hardness of the biofoam also increased with the filler loading showed the optimum value at the optimum fiber content, which is Shore D 35 at 6% of EFB loading.

Table 1. Properties of the biofoam

EFB Loading, %	0	3	6	9	12
Molded density, kg/m^3	168	170	170	166	164
Rheological index, cm/g	0.3	0.6	0.7	0.7	0.7
Cream time, s	17	16	22	16	19
Fiber time, s	35	36	53	33	42
Take free time, s	44	49	72	47	54
Rise time, s	91	88	100	83	77
Hardness, Shore D	28	32	35	26	21

The mechanical properties of the biofoam produced from the polyol show interesting results due to the functionality of the polyol itself. The dimensional

stability of the biofoam was showing good performances due to the percentage of volume change of the foam are very small quantity. Almost all of the biofoam shows the percentages of volume change are less than 1%. Figure 1 indicates the compressive strength and the compression modulus of the biofoams. From the Figure 1, it shows the compressive strength of the foams increases up to 6% part by weight and decreased with further addition of EFB fibers.

The surfaces of cellulose fibers are hydrophilic and it would be expected that enhanced compatibility between fibers and PU matrix. This is in relation to the molecular structure of the EFB fibers itself where the present of the hydroxyl group which will be attacked by the isocyanate group from the crude isocyanate. This will improved the wetting of the fiber by the PU's matrix, then lead to a stronger interfacial bond without presents coupling agent. It will be more efficient stress transfer between the fibers as a load is applied. The compression modulus decreased at 12 % loading due to the softening behavior at higher strain values in the stress-strain response. It is attributed to the debonding of EFB fibers, which is predominant at higher loading.

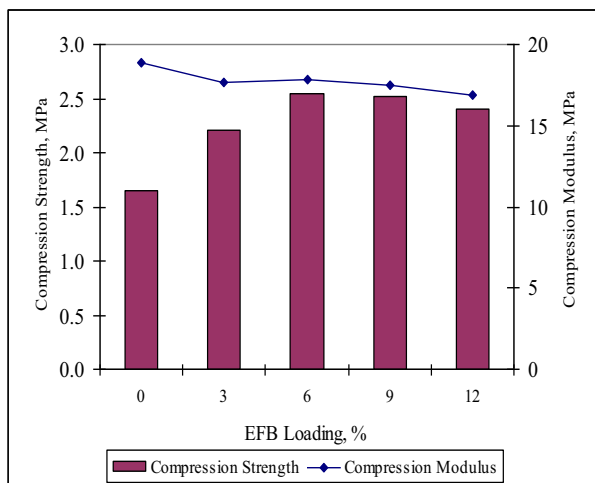


Figure 1. Compressive strength and compression modulus of the biofoam

The effect of addition EFB fibers on tensile strength and tensile modulus were shown in Figure 2. The tensile strength increased up to 9% of EFB fibers loading and decreased with further addition. In tensile strength, there are two major competing phenomena affecting. The increase in the tensile strength of the composites is due to load sharing by the EFB fibers. At the same time, introduction of the filler in a matrix causes localized stress intensification. As the filler of EFB increases, the stress concentration increases. These high stress initiate debonding as dewetting occurs, load sharing by the EFB fibers decreases. The debonded region acts essentially as a void and reduces the tensile strength. The effect of dewetting on tensile strength is predominant only at higher loading of fibers.

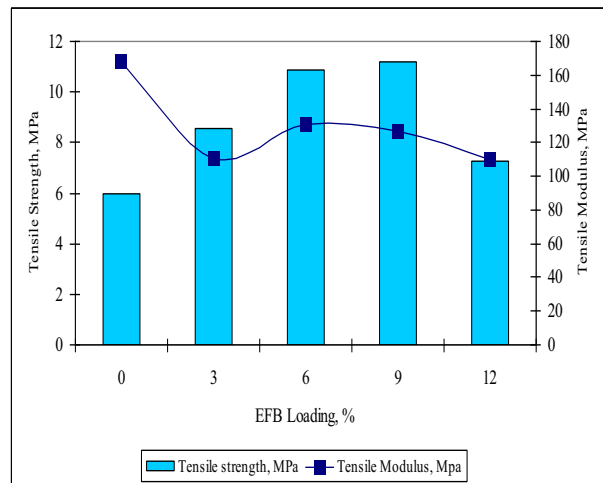


Figure 2. Tensile strength and tensile modulus of the biofoam

Figure 3 depict the effect of EFB fibers loading on the MOE and MOR respectively. The increment in the MOE and MOR at the lower loading of the natural polymer can be attributed the incorporation of more aromatic rings into PU system, which leads to an increase in chain stiffness. While, the decrement after 9% loading is due to the increasing EFB content, which turns reducing the matrix content. Thus, the matrix formation would be reduced according the effect of dewetting is predominant at higher loadings.

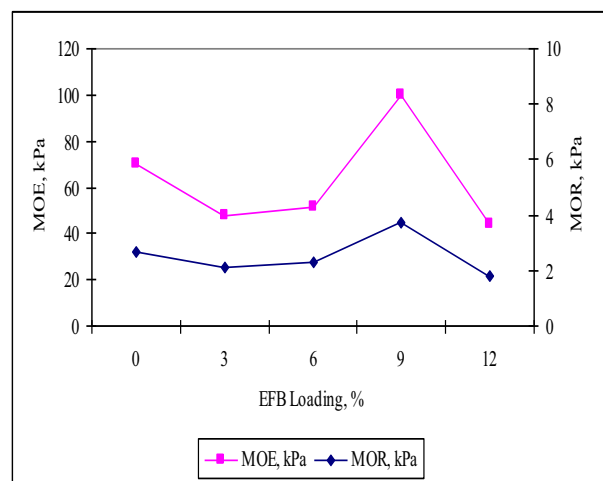


Figure 3. Effect of the MOR and MOE of biofoam

Impact fracture of the medium density biofoam could be a combination of fiber pull out and fiber breakage. The work of debonding and pull out needs more energy and thus the impact energy increases on easy pull out that occurs in the biofoam. Figure 4 shows the unnotched Izod impact strength of the biofoams. The addition of EFB fibers enhanced the impact strength about 50% at 6% EFB fibers loading and decreased with the further addition of EFB fibers. It can be explained when at lower loading (<6%), fibers are found embedded in the matrix and hence fiber breakage and fiber pull out occur on application of a sudden force. But, at higher loadings, fibers to fibers contacts increases and fiber breakage will be predominant failure mechanism. The inter fiber

interaction decreases the effective stress transfer between the fiber and matrix.

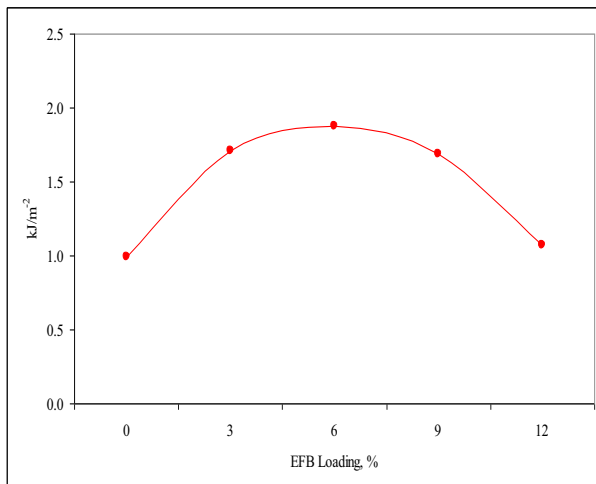


Figure 4. Impact strength of biofoam

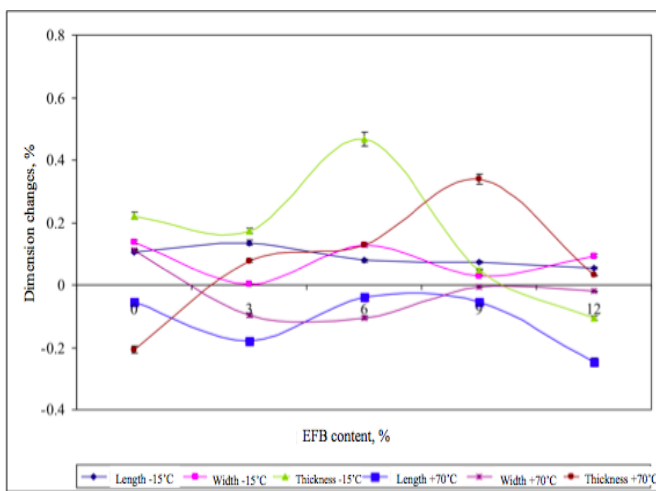


Figure 5. Dimensional stability of biofoam

Dimensional stability is also of great importance for the applications of PU foam in various fields. Figure 5 shows the dimensional stability of biofoams at -15°C and 70°C . The dimensional stability test was carried out to observe any severe expansion and shrinkage problems on the foam. This is to ensure the stability upon heat or cold temperature. Since this property depends on the cell shape and size, the thickness of the foam is the major part that is of concern, as it represents the foam rise direction. The larger the size of the fibre, the higher the percentage of linear change in the foam dimensions as a function of thickness is. Figure 5 shows the values were much smaller than the requirements of some commercial standards (percentage of change in linear dimension should be lesser than 1 and 3% for testing conditions of -15°C and 70°C for 24 h, respectively) indicating the excellent dimensional stabilities of PU biofoams. However, the thickness values showing deteriorative values compared to length and width. This is due to tearing of the cell wall during expansion of the foam and resulted in a faster diffusion rate of carbon dioxide produced during

the polymerization, outward to be replaced by the air inward.

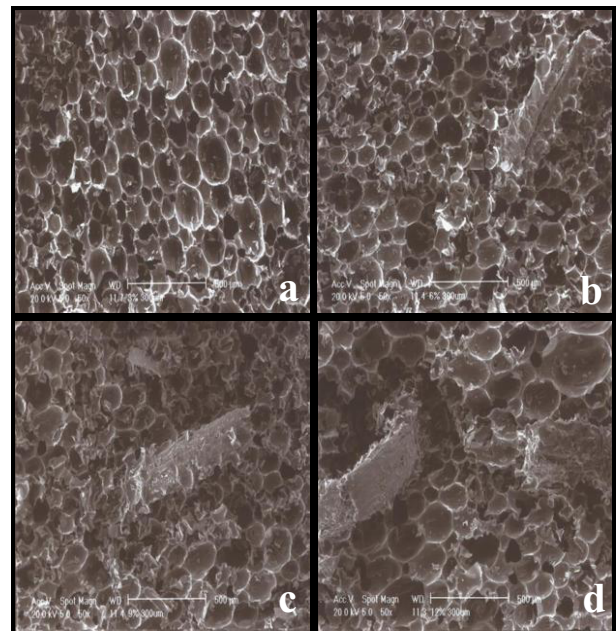


Figure 6. SEM micrograph of biofoams at 50x (a) 3% (b) 6% (c) 9% (d) 12%

Typical structure of the biofoams as shown in Figure 6 (a), (b), (c) and (d) were observed using SEM. Cell edges and cell walls are distinctly visible with almost uniform cell structures throughout. From Figure 6, biofoams exhibit that the structure cells is not exactly spherical, but quite polygon. It is because the ratio of the carbon dioxide volume phase increased rapidly, thus the cells intend to form the hexagonal structure. The addition of the EFB fibers in the low loading, clearly showed that EFB does not effected the growth of the cells structure. Which are the EFB fibers are embedded in the PU foam structure and filled the cells. But at the higher loading, the EFB fibers started to distract the cell edges and the cell walls resulted the low mechanical properties. Figure 6 shows some occurrence of fibre pull-out. Less matrix is deposited per unit area for samples in this biofoams as EFB used were larger particle size; in which offering smaller surface area. This would explain why fibre pull-out are quite obvious in these figure.

4 Conclusion

The study showed that this polyol that is derived from PKO with the functionality 3.0 can produced the medium density polyurethane rigid foam with acceptable mechanical properties. The usages of the EFB as filler also demonstrated a good results due to the compression tensile, MOE, MOR and impact properties of the biofoam. In terms of application, this composite is most suitable in structures where stiffness and dimensional stability is of prime importance but only a secondary choice to areas where structural strength is more vital than component rigidity.

References

1. G. Woods. The ICI Polyurethane Handbook. John Wiley & Sons: New York. (1990)
2. Cordero, A. I., Amalvy, J. I., Fortunati, E., Kenny, J. M. & Chiacchiarelli, L. M, *Carb. Polym.* **134** (2015)
3. Septevani, A. A., Evans, D. A. C., Chaleat, C. & Martin, D. J. *Inds Crops And Products.* **66** (2015)
4. Jinjie G, Wi Z, Zhenrong. G, Wenjun, L. & Kokki, S, *J. App. Polym. Sc.* **77** (2000)
5. Pourjavadi, A., Rezai, N. & Zohuriaan-M, M. J., *J. App. Polym. Sc.* **68** (1998)
6. Badri, K. H, Ahmad, S. H dan Zakaria S. 2000. *J. Of. Material Sc. Letters.* **19**:1355
7. Ali, E. S, & Ahmad, S. *Composites Part B: Engineering.* **43**, 7 (2012)
8. Badri, K. H, & Ahmad, S. H. *J. Mater. Sci.* **39** (2004)
9. Rozman, H. D, Tay, G. S, Bakar, A. A, Kumar, R. N. *European Polym. J.* **30** (2001)
10. Sreekala, M. S, George J, Kumaran, M. G, Thomas, S. *Composites Sc. and Technology.* **62** (2001)
11. Xiaoya, C, Qipeng, G, Yonghi, M. *J. App. Polym. Sc.* **69** (1998)